

Measurement of the $f_1(1285) \rightarrow \pi^+ \pi^- \pi^0$ decay

V. Dorofeev¹, A. Ekimov¹, Yu. Gouz¹, A. Ivashin¹, I. Kachaev¹, A. Karyukhin¹, Yu. Khokhlov^{1,2,a}, V. Konstantinov¹, V. Matveev¹, V. Nikolaenko¹, B. Polyakov¹, D. Ryabchikov¹, N. Shalanda¹, M. Soldatov¹, A.A. Solodkov¹, A.V. Solodkov¹, O. Solovianov¹, and A. Zaitsev^{1,2}

¹ Institute for High Energy Physics, Protvino, Russia

² Moscow Institute of Physics and Technology, Moscow, Russia

Received: 17 October 2010 / Revised: 29 March 2011

Published online: 30 May 2011

© The Author(s) 2011. This article is published with open access at Springerlink.com

Abstract. The isospin symmetry-breaking (ISB) decay $f_1(1285) \rightarrow \pi^+ \pi^- \pi^0$ has been studied at the VES facility. The branching ratio is measured: $\frac{BR(f_1 \rightarrow \pi^+ \pi^- \pi^0)}{BR(f_1 \rightarrow \eta \pi^+ \pi^-)} = 0.86 \pm 0.16^{+0.70}_{-0.20}\%$. An upper limit for the f_1 decay into $\rho(770)\pi$ is obtained: $BR(f_1(1285) \rightarrow \rho^+ \pi^- \pi^+) < 0.31\%$ at 95% CL.

1 Introduction

In this paper we study the isospin symmetry-breaking (ISB) decay $f_1(1285) \rightarrow 3\pi$. There is a number of ISB decays observed so far. They are driven mainly by the difference of light quark masses $\Delta m = m_d - m_u$ [1–3]. The $\omega \rightarrow \pi\pi$ and $\eta \rightarrow 3\pi$ are among the most known, with underlying $\Delta I = 1$ transitions $\omega \leftrightarrow \rho$ and $\eta \leftrightarrow \pi$ determined by a universal scale [4].

The decay $f_1(1285) \rightarrow 3\pi$ can proceed through several different mechanisms. One of them, $f_1(1285) \leftrightarrow a_1(1260)$ mixing, is possible assuming that the universality [4] can be extended to the axial meson sector. Another mechanism is the direct decay $f_1 \rightarrow 3\pi$, however such “contact” contributions are expected to be small.

An alternative mechanism, taking into account the dominance of the decay channel $f_1 \rightarrow a_0(980)\pi$, was suggested in [5,6]. It is based on the predicted [7] $a_0(980) \leftrightarrow f_0(980)$ mixing through their couplings to kaons. Qualitatively, the cancellation of loops with virtual $K\bar{K}$ pairs is not perfect because of the difference of masses of charged and neutral kaons. The overall ISB amplitude is significant in the narrow mass region between the corresponding $K\bar{K}$ thresholds due to the proximity of the masses of both resonances. Following [5,6], it is expected that the decay $f_1 \rightarrow \pi^+ \pi^- \pi^0$ (or $3\pi^0$) is also enhanced in a narrow region of the $m_{\pi\pi}$ close to $2m_K$.

Some theoretical aspects of the $a_0 \leftrightarrow f_0$ mixing are discussed in [8]. Along with the experimental approaches referenced there (see also [9]), the study of $f_1 \rightarrow 3\pi$ decay can give valuable information about this phenomenon.

2 Search for the decay $f_1(1285) \rightarrow \pi^+ \pi^- \pi^0$

The diffractive reaction $\pi^- N \rightarrow \pi^- f_1(1285)N$ representing a rich source of the f_1 -mesons at relatively low background was used for the search. It has been studied at VES in details in the dominant decay mode $f_1 \rightarrow \eta \pi^+ \pi^-$ [10–12], and it serves as a reference for the analyses tuning and normalization.

This study is based on the data collected in several expositions at beam momenta of 27, 37 and 41 GeV/c on a Be target. The VES detector [13] is a wide-aperture magnetic spectrometer equipped with a lead-glass electromagnetic calorimeter and Cherenkov detectors for identification of beam and charged secondary particles.

The π^0 -mesons in the reaction for the search for $f_1 \rightarrow 3\pi$ signal (called here “signal reaction”),

$$\pi^- N \rightarrow N \pi^+ \pi^- \pi^- \pi^0, \quad (1)$$

and the η in the reaction with main decay mode $f_1 \rightarrow \eta \pi \pi$ (“reference reaction”)

$$\pi^- N \rightarrow N \pi^+ \pi^- \pi^- \eta, \quad (2)$$

were detected in the $\gamma\gamma$ mode.

The event-selection criteria for the reference reaction are described in [10,11]. Similar procedure was used for the $(\pi^+ \pi^- \pi^- \pi^0)$ system. Here the invariant mass of two photons was requested to be in the range (0.105, 0.165) GeV/c². The fraction of background in $\gamma\gamma$ mass spectra was estimated as 24% and 36% for reactions (1) and (2), respectively. A kinematical 1C-fit of the photons energy to the neutral meson mass has been performed for both reactions.

^a e-mail: Yury.Khokhlov@ihep.ru

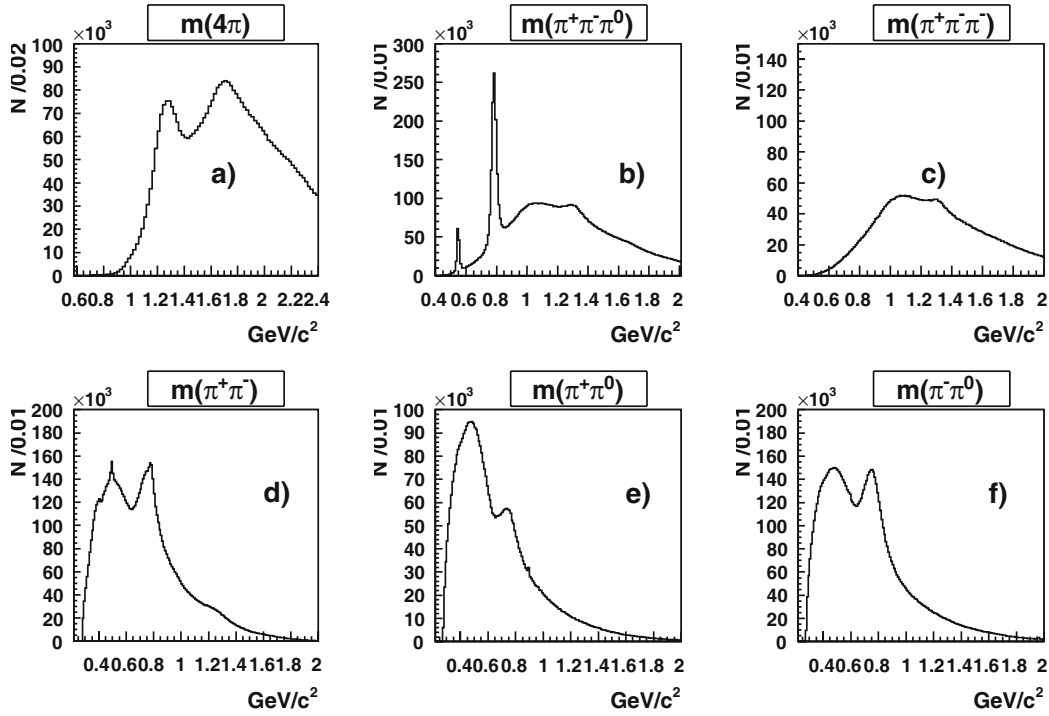


Fig. 1. Invariant masses for $(\pi^+\pi^-\pi^-\pi^0)$ system: a) $m_{4\pi}$, b) $m_{\pi^+\pi^-\pi^0}$, c) $m_{\pi^+\pi^-\pi^-}$, d) $m_{\pi^+\pi^-}$, e) $m_{\pi^+\pi^0}$, f) $m_{\pi^-\pi^0}$.

Figure 1 shows various invariant-mass spectra for the selected $\pi^+\pi^-\pi^-\pi^0$ sample of the reaction under study. The $b_1(1235)$ signal (see below) is seen in the 4π mass distribution (fig. 1a). Prominent peaks from the $\omega(782)$ and the η are observed in the $(\pi^+\pi^-\pi^0)$ subsystem (fig. 1b), the former being associated mainly with the $b_1(1235)$ production. An accumulation of events is seen also in the mass region of the $f_1(1285)$ and $a_2^0(1320)$ mesons. The three $\pi\pi$ subsystems are dominated by broad ρ -meson peaks (fig. 1d–1f); in addition, in the $\pi^+\pi^-$ mass spectrum (fig. 1d) narrow peaks of K_s^0 and ω -mesons are seen.

The $f_1(1285)\pi^-$ final state is produced diffractively [10–12], at low momentum transfer squared $t' = |t| - |t_{max}|$. Other processes with $\pi^-\pi^+\pi^-\pi^0$ in the final state, which are the background to the one under study, proceed via odd G-parity exchange and in general have wider distributions on t' . The ratio of the t' -distributions for the reaction (2) to that for (1) (fig. 2) clearly demonstrates the forward diffractive peak. To increase the signal-to-background ratio, the events at low momentum transfer squared, $t' < 0.04$, were selected. In addition, the non-coherent events with target nucleus fragmentation were rejected on the basis of signal in the target guard system¹.

¹ This system is a double-layered set of counters, scintillator plates in the inner layer and lead-scintillator “sandwiches” in the outer one, surrounding the target. It is sensitive to both charged particles and photons coming from the target. It covers mainly the backward hemisphere of the beam-target scattering, with its opening ($\sim \pm 150$ mrad) matching the spectrometer acceptance.

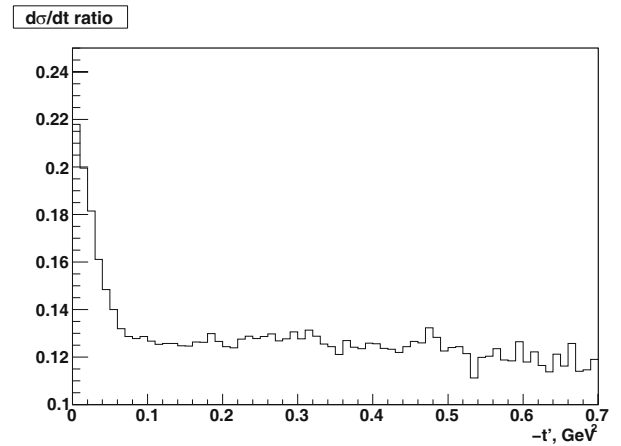


Fig. 2. Ratio of t' -distribution for $\pi^-N \rightarrow N\pi^+\pi^-\pi^-\eta$ to that for $\pi^-N \rightarrow N\pi^+\pi^-\pi^-\pi^0$.

However, the suppression of the $\omega\pi^-$ and $\eta\pi^-$ systems is insufficient with the t' cut, because $b_1^-(1235) (\rightarrow \omega\pi^-)$ and $a_2^-(1320) (\rightarrow \eta\pi^-)$ are abundantly produced at low t' . To further improve the event selection, an additional cut was applied to the events of “signal reaction”: both $\pi^+\pi^-\pi^0$ combinations were requested to have $m_{\pi^+\pi^-\pi^0} > m_\omega + 1.5\sigma_\omega \approx 0.810 \text{ GeV}/c^2$. Here m_ω is the table mass of the $\omega(782)$ and $\sigma_\omega \approx 18 \text{ MeV}/c^2$ is the experimental width of its peak.

The $f_1 \rightarrow \eta\pi^+\pi^- \rightarrow \gamma\gamma\pi^+\pi^-$ signal in the reference reaction (2) at low t' is shown in fig. 3. The fit with the Breit-Wigner function and polynomial background gives $N_\eta = (108 \pm 2) \cdot 10^3$ events in the peak.

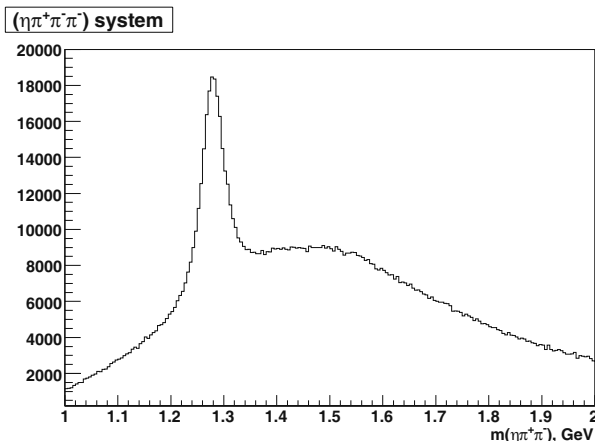


Fig. 3. The $m_{\eta\pi^+\pi^-}$ spectrum (two entries per event) in the reaction (2) at $t' < 0.04 \text{ GeV}^2/c^2$.

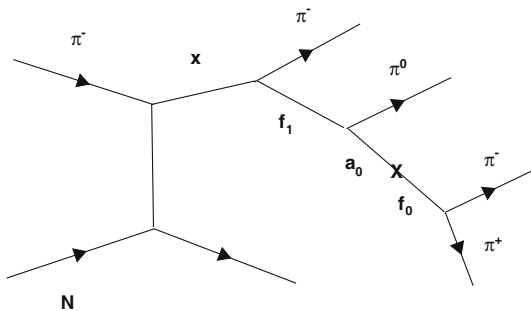


Fig. 4. Schematic diagram of the sought process.

The results of the partial-wave analysis [12] show that the $f_1\pi^-$ is dominantly produced in a state with $J^{PC}M\eta = 1^{++}0^+$, here M and η denote the spin projection number and the exchange “naturalness”, respectively. The f_1 and π^- are therefore produced in P -wave. The f_1 decays in its turn predominantly into a pion and $a_0(980)$ ($f_0(980)$) for reference (signal) reaction, again with orbital momentum $L = 1$. Finally the a_0 (f_0) decays into a $\eta\pi$ ($\pi\pi$) pair in S -wave. The signal process is shown schematically in fig. 4.

The angular part of the amplitude for the dominant $1^{++}0^+$ state in the $f_1\pi^-$ system (see appendix A) is expressed in a compact way using specific angles:

$$|A| = \frac{3}{\sqrt{2}} |\sin\theta_1 \cdot \sin\theta_2 \cdot \sin(\phi_0 - \phi_2)|. \quad (3)$$

Here θ_1 is the polar angle of the $f_1(1285)$ momentum in the Gottfried-Jackson system; θ_2 is the angle between this momentum and the momentum of η (π^0) in the f_1 center-of-mass system. ϕ_2 and ϕ_0 are azimuthal angles of the momenta of η (π^0) in the f_1 c.m.s. and the beam particle in the $f_1\pi^-$ c.m.s., measured in the plane, perpendicular to the momentum of f_1 in the $f_1\pi^-$ c.m.s.

The event-by-event weight $W = |A|^2$ can be used to enhance the f_1 signal. It is demonstrated in fig. 5d which shows the ratio of $(\eta\pi^+\pi^-)$ invariant-mass spectrum weighted with the W (corrected for angular acceptance) to the unweighted one.

The $m_{\pi^+\pi^-\pi^0}$ distribution for the signal sample is presented in fig. 5a. A broad ($> 100 \text{ MeV}/c^2$) peak at $\approx 1300 \text{ MeV}/c^2$ is observed, which cannot be attributed unambiguously either to the $a_2(1320)$ or to the $f_1(1285)$ alone. To separate the signal of f_1 , the angular weight W was applied to this spectrum (fig. 5b). The effect is demonstrated with the ratio of these two (fig. 5c): a certain enhancement in the $f_1(1285)$ mass region becomes visible on top of a smooth background.

The enhancement becomes more prominent if we add a requirement on the two-pion subsystem mass: $0.97 < m_{\pi^+\pi^-} < 1.0 \text{ GeV}/c^2$ (fig. 5e). The fit with the sum of a Gaussian and a linear background in the mass interval $1.18\text{--}1.40 \text{ GeV}/c^2$ yields for the peak parameters $m = 1276 \pm 4$ and $\sigma = 25 \pm 3 \text{ MeV}/c^2$. The peak position and width agree with expectations for the $f_1(1285)$ smeared by the detector resolution. The statistical significance of the peak is 7.8 standard deviations, $\chi^2/\text{ndf} = 53/40$.

As a cross-check, the same angular weighting procedure was applied to other mass spectra: $m_{\pi^+\pi^-\pi^0}$ for the same event sample (fig. 5f) and $m_{\pi^+\pi^-\pi^0}$ for the event sample at large t' (not shown). As expected, no enhancement around $f_1(1285)$ mass is seen in these cases.

We can conclude that the application of angular weighting procedure, corresponding to known $f_1\pi^-$ production and decay properties, indeed extracts the peak at the f_1 mass in the $m_{\pi^+\pi^-\pi^0}$ spectrum. The peak is associated with narrow interval on $m_{\pi^+\pi^-}$ in the region of the $f_0(980)$ mass. This is giving us confidence that the decay $f_1 \rightarrow \pi^+\pi^-\pi^0$ is indeed observed, and its pattern does not contradict the model [5–7] predictions.

The probability of this decay was evaluated using a conventional bin-filtering procedure, which is described below. The signal in the $\pi^+\pi^-$ mass spectrum will be denoted below as “ f_0 ”, although its parameters can be determined by the $f_1 \rightarrow 3\pi$ decay dynamics and do not necessarily coincide with those of the $f_0(980)$ -meson (see [5–7]).

The mass spectrum $m(\pi^+\pi^-)$ at the f_1 peak ($1.280 < m(\pi^+\pi^-\pi^0) < 1.290 \text{ GeV}/c^2$) was analyzed (fig. 6). Apart from the K_s^0 and ρ - ω peaks, a narrow bump is seen around $m(\pi^+\pi^-) \sim 985 \text{ MeV}/c^2$. To determine the background under this bump, the spectrum was fitted in the full mass range except the region of interest, $0.93\text{--}1.03 \text{ GeV}/c^2$. The fitting function was a polynomial multiplied by the phase space for a decay $m_{3\pi} \rightarrow m_{2\pi} + m_\pi$, plus relativistic P -wave Breit-Wigner for the $\rho(770)$ in the Ross-Stodolsky parameterization [14,15] with skewness parameter $\alpha = 3.8$, plus Gaussians for K^0 and $\omega(782)$. The masses of narrow objects turned out to be compatible with the PDG values [16]; their widths which are determined mainly by the detector resolution are in agreement with the simulation results. The background function obtained from the fit was then subtracted from the experimental spectrum.

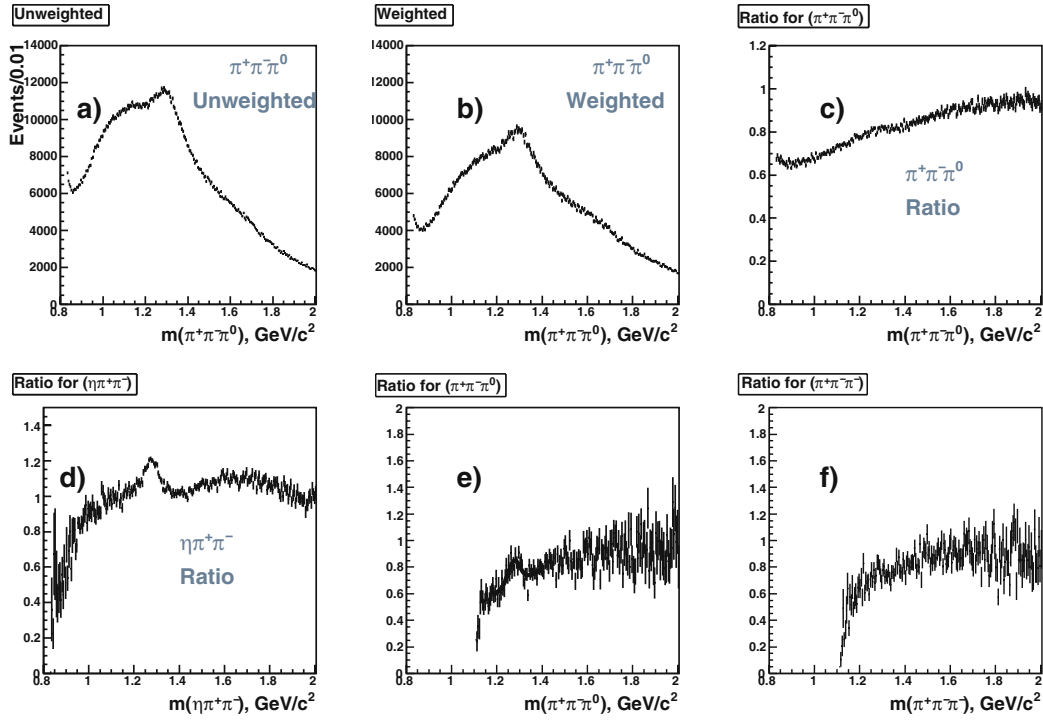


Fig. 5. The effect of the weighting (see text) on three-meson mass spectra: a) $m_{\pi^+\pi^-\pi^0}$ spectrum, low t' ; b) as in a) but weighted; c) spectra ratio b) to a); d) “weighted/unweighted” spectra ratio for $\eta\pi^+\pi^-$ at low t' ; e) like in c) for events with $0.97 < m_{\pi^+\pi^-} < 1.00 \text{ GeV}/c^2$; f) like in e) but for charged subsystem $\pi^+\pi^-\pi^-$.

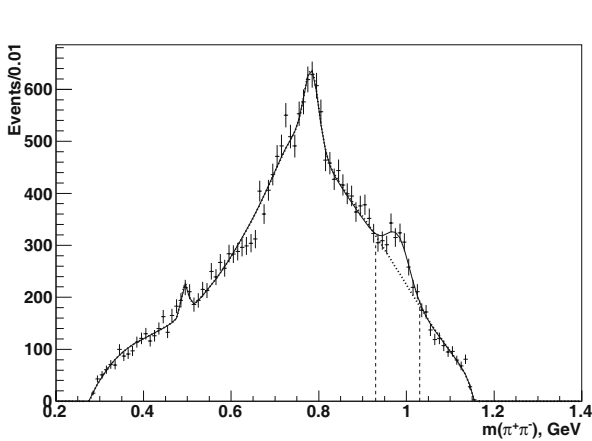


Fig. 6. The $m_{\pi^+\pi^-}$ spectrum (histogram) for $1.28 < m_{\pi^+\pi^-\pi^0} < 1.29 \text{ GeV}/c^2$, with the fit result (solid line). The background function (dotted line) and signal range (dashed) are also shown.

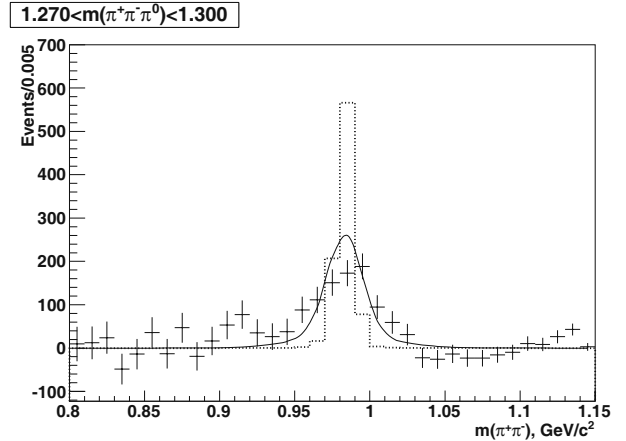


Fig. 7. The $m_{\pi^+\pi^-}$ spectrum (histogram) after background subtraction for $1.27 < m_{\pi^+\pi^-\pi^0} < 1.30 \text{ GeV}/c^2$. The typical $m_{\pi^+\pi^-}$ spectrum for the $a_0(890) \leftrightarrow f_0(980)$ mixing model [5–7] is shown, without (dotted line) and with (full line) detector resolution smearing.

The same fitting procedure followed by background subtraction was performed also for two adjacent 10 MeV bins on $m_{\pi^+\pi^-\pi^0}$, 1.27–1.28 and 1.29–1.30 GeV/c^2 . The sum of the three distributions after background subtraction, with a clear “ f_0 ” peak, is shown in fig. 7. The Gaussian parameters of the peak are determined as follows: $m = 0.982 \text{ GeV}/c^2$ and $\sigma = 0.025 \text{ GeV}/c^2$. The peak is somewhat broader than expected within the framework

of the model [5–7], taking into account the detector resolution ($\sigma \sim 16 \text{ MeV}/c^2$), and is compatible with $f_0(980)$ PDG parameters.

The bin-filtering procedure for the f_1 -meson signal extraction was then performed for 30 10 MeV bins on $m_{3\pi}$ in the range of 1.15–1.45 GeV/c^2 , with position and width of the “ f_0 ” peak fixed to the values determined above. The

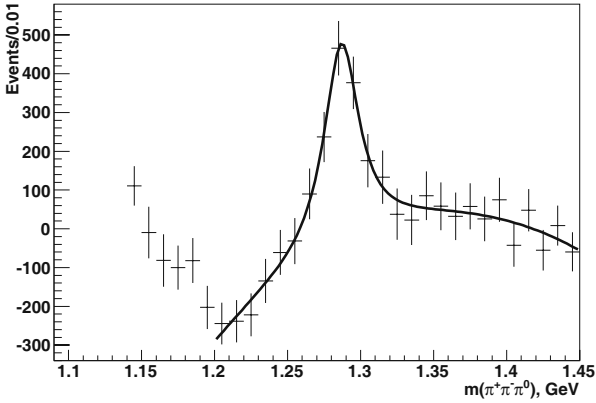


Fig. 8. The fitted number of “ f_0 ” events as a function of $m_{\pi^+\pi^-\pi^0}$; the superimposed curve corresponds to the sum of a Breit-Wigner function and a second-order polynomial.

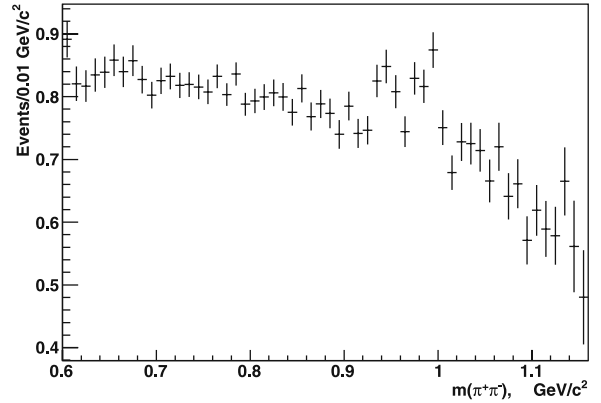


Fig. 9. The ratio of weighted to unweighted $m_{\pi^+\pi^-}$ spectra for $1.26 < m_{\pi^+\pi^-\pi^0} < 1.31 \text{ GeV}/c^2$.

numbers of events in the “ f_0 ” peak obtained from the fit in each $m_{3\pi}$ bin, along with their errors, are shown in fig. 8 as a function of $m_{3\pi}$.

The obtained dependence is fitted with a sum of a Breit-Wigner function and a 2nd-order polynomial. The resulting peak parameters, $m = 1287 \pm 2 \text{ MeV}/c^2$ and $\Gamma = 30 \pm 6 \text{ MeV}/c^2$, are in agreement with the $f_1(1285)$ parameters. It should be noted that the experimental width of the f_1 peak is less than that of the “daughter” “ f_0 ” in the $\pi^+\pi^-$ subsystem; this proves that the “ f_0 ” width is not dominated by the detector resolution, which disagrees with the model with very narrow “ f_0 ”.

The total number of events in the peak is $N_{\pi^0} = 2300 \pm 400$. Taking into account the ratio of the detection efficiencies for the f_1 decays into $\pi^+\pi^-\pi^0$ and $\pi^+\pi^-\eta$, $R = \varepsilon(3\pi^+\pi^-\pi^0)/\varepsilon(3\pi^+\pi^-\eta) = 0.95 \pm 0.05$, we obtain the ratio of branchings:

$$\frac{BR(f_1 \rightarrow “f_0”\pi^0 \rightarrow \pi^+\pi^-\pi^0)}{BR(f_1 \rightarrow \eta\pi^+\pi^-) \cdot BR(\eta \rightarrow \gamma\gamma)} = \frac{N_{\pi^0}}{N_{\eta}R} = (2.2 \pm 0.4(\text{stat}) \pm 0.5(\text{syst}))\%. \quad (4)$$

The statistical error is dominated by the N_{π^0} fit error. The systematic uncertainty was estimated by varying: the “ f_0 ” peak width (down to the resolution limit of $16 \text{ MeV}/c^2$, see, however, below), the $f_1(1285)$ shape (Gaussian or Breit-Wigner for both channels), the order of polynomials for the background description, and the ρ -meson parameterization.

Yet another indication to broad “ f_0 ” peak disagreeing with the model [5–7] predictions was found. Namely, the angular weighting of events was done in another way. It was applied to events with a mass of neutral combination of three pions lying within $1.260 < m_{\pi^+\pi^-\pi^0} < 1.310 \text{ GeV}/c^2$, and the effect on the $\pi^+\pi^-$ mass spectra was studied. The ratio of weighted to unweighted $m_{\pi^+\pi^-}$ distributions is shown in fig. 9. It is almost flat, with the “ f_0 ” peak at $\sim 980 \text{ MeV}/c^2$ as expected. The peak is how-

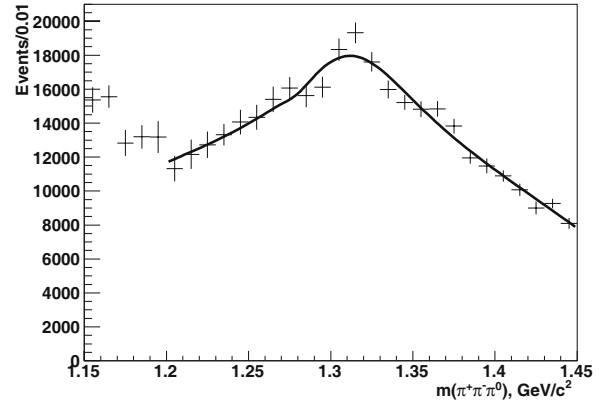


Fig. 10. The number of ρ^{++} events from fits in $m_{\pi^+\pi^-\pi^0}$ intervals (points with errors) with the fitting function superimposed (see text).

ever even broader than in fig. 7, and extends down to $\approx 0.94 \text{ GeV}/c^2$.

For this reason, a wider range of mass and width for the “ f_0 ” Gaussian in the bin-filtering procedure was explored for the evaluation of the systematic error. When the Gaussian extends to the low-mass tail of the $m_{\pi^+\pi^-}$ bump, the fitted number of events increases. In the extreme case of $\sigma(\text{“broad } f_0\text{”}) = 40 \text{ MeV}/c^2$, the resultant peak in $m_{3\pi}$ has $N_{\pi^0} \approx 4 \cdot 10^3$ events and is compatible with the $f_1(1285)$. This gives $BR(f_1 \rightarrow \text{“broad } f_0\text{”}\pi^0 \rightarrow \pi^+\pi^-\pi^0)/(BR(f_1 \rightarrow \eta\pi^+\pi^-) \cdot BR(\eta \rightarrow \gamma\gamma)) \approx 4.0\%$.

2.1 Search for $f_1(1285) \rightarrow \rho^{+-}\pi^{-+}$

A search for a possible $f_1 \leftrightarrow a_1$ mixing was also performed, assuming $\rho^{+(-)}\pi^{-(+)}$ final states. The number of $\rho^{+(-)}$ decay events was determined with bin-by-bin fit of $m_{\pi^{+(-)}\pi^0}$ spectra in $m_{3\pi}$ intervals. The total ρ^{+-} intensity as a function of $m_{\pi^+\pi^-\pi^0}$ is shown in fig. 10. No enhancement at the $f_1(1285)$ mass is observed.

This spectrum was fitted with a sum of two Breit-Wigner functions with fixed masses and widths for f_1 and $a_2(1320)$ plus a 2nd-order polynomial for the background. The fit gives (with $\chi^2/\text{ndf} = 31./21$) $N_{\rho^{+-}} = -2700 \pm 2400$ events of the $f_1 \rightarrow \rho^{+-}\pi^{-+}$ decay, which corresponds to $BR(f_1 \rightarrow \rho^{+-}\pi^{-+}) = (-0.34 \pm 0.31)\%$. From this we can derive the upper limit for the branching fraction

$$BR(f_1(1285) \rightarrow \rho^{+-}\pi^{-+}) < 0.31\% \quad (5)$$

at the 95% CL.

The intensity of the $f_1 \rightarrow a_1$ transition is determined by the polarization operator $\Pi_{f_1 a_1}$ [17]:

$$\begin{aligned} BR(f_1 \rightarrow \rho\pi) &= \\ \frac{\Gamma_{a_1 \rightarrow \rho\pi}}{\Gamma_{f_1}} \frac{\Pi_{f_1 a_1}^2}{|m_{f_1}^2 - m_{f_1}^2 - i(m_{f_1}\Gamma_{f_1} - m_{a_1}\Gamma_{a_1})|^2} \\ &\approx \frac{\Pi_{f_1 a_1}^2}{m_{f_1}^2 \Gamma_{f_1} \Gamma_{a_1}}. \end{aligned}$$

From (5) we obtain:

$$|\Pi_{f_1 a_1}| < 0.0087 \text{ GeV}^2 \text{ for } \Gamma_{a_1} = 600 \text{ MeV}.$$

It is compatible with the universal scale of ISB [4]:

$$\Pi_{\rho\omega} \approx \Pi_{\eta\pi} \approx -0.005 \text{ GeV}^2.$$

3 Model calculation for $a_0 \rightarrow \pi^+\pi^-$ transition and discussion

We compute the model branching for a mixing transition $R \rightarrow X \rightarrow c d$ following [18]. There is a large variety of theoretical and experimental values for the relevant parameters of scalar mesons in the literature: sets A to H from [19] are taken as an example in what follows.

The highest value for the $a_0 \rightarrow \pi\pi$ branching among the quoted sets of parameters is obtained with the set C for the $K\bar{K}$ molecular model of two scalars:

$$BR(a_0 \rightarrow \pi^+\pi^-) = 0.79\%.$$

For the self-consistency of the comparison, the reference branching fraction $BR(a_0 \rightarrow \eta\pi)$ should also be calculated with the same input parameters. For C this yields $BR(a_0 \rightarrow \pi^+\pi^-)/BR(a_0 \rightarrow \eta\pi^0) = 1.58\%$. Incidentally, the computed $BR(a_0 \rightarrow K^+K^-)/BR(a_0 \rightarrow \eta\pi^0) = 20\%$ is by a factor of 2 larger than the world average [16].

As a stability check, the full decay chains $f_1 \rightarrow a_0\pi \rightarrow \eta\pi\pi(K\bar{K}\pi)$ and $f_1 \rightarrow a_0\pi \rightarrow f_0\pi \rightarrow \pi\pi\pi$ were calculated within the model accounting for a Breit-Wigner line shape of the f_1 . The momentum-dependent form factors $\propto (p/p_0)^2$ and $\propto (1 - \exp(-(p/p_0)^2))$ in the P -wave decay $A \rightarrow SP$ were tried. The resulting branching fractions follow those of the a_0 , precisely for the mixing transition and with some ten percent variations for the reference channel.

The measured branching fraction from (4)

$$BR(f_1 \rightarrow "f_0"\pi \rightarrow \pi^+\pi^-\pi^0) = (0.30 \pm 0.055(\text{stat}) \pm 0.068(\text{syst}) \pm 0.029(BR))\%, \quad (6)$$

where the last error comes from the uncertainty in the reference partial width $x_7 = \Gamma_7/\Gamma$ ([16], p. 670): $BR(f_1 \rightarrow \eta\pi^+\pi^-) = \frac{2}{3}x_7 = \frac{2}{3}(0.52 \pm 0.05)$.

Assigning the origin of the decay $f_1 \rightarrow "f_0"\pi \rightarrow 3\pi$ entirely to the $a_0 \rightarrow f_0$ transition regardless of its specific mechanism, it is translated to

$$BR(a_0^0(980) \rightarrow \pi^+\pi^-) = (2.0 \pm 0.6 \pm 0.4(BR))\%.$$

For the calculation the $BR(f_1 \rightarrow a_0^0\pi^0) = 1/3 x_8 + 1/3 x_{10} = 0.15 \pm 0.023$ ([16]) is used. The uncertainty from branchings accounts for table errors δ_i of x_i ($i = 7, 8, 9$) and their correlation coefficients $\rho_{i,j}$, with $x_7 \equiv x_8 + x_9$ and

$$\rho_{7,8} = \frac{1 + \rho_{8,9}\delta_8/\delta_9}{\sqrt{1 + (\delta_8/\delta_9)^2 + 2\rho_{8,9}\delta_8/\delta_9}} = 0.16.$$

The contribution from relatively small δ_{10} was evaluated and neglected. Statistical and systematic errors are added in quadrature. Within the model [5–7], obtained large value of branching is feasible only marginally.

In addition, the large width of the two-pion structure, with its lower mass ($m_{\pi^+\pi^-} \lesssim 0.97 \text{ GeV}/c^2$) enhancement of comparable size, is beyond the model and possibly points to another mechanism in the decay $f_1(1285) \rightarrow \pi^+\pi^-\pi^0$.

4 Conclusions

The isospin symmetry-breaking decay $f_1(1285) \rightarrow \pi^+\pi^-\pi^0$ is observed. The ratio of branchings is determined:

$$\begin{aligned} \frac{BR(f_1 \rightarrow "f_0(980)"\pi^0 \rightarrow \pi^+\pi^-\pi^0)}{BR(f_1 \rightarrow \eta\pi^+\pi^-)} &= \\ (0.86 \pm 0.16(\text{stat.}) \pm 0.20(\text{syst.}))\%, & \quad (7) \end{aligned}$$

where " $f_0(980)$ " stands for a probably S -wave structure centered at $m_{\pi^+\pi^-} \approx 0.98 \text{ GeV}/c^2$. This gives

$$BR(f_1 \rightarrow "f_0(980)"\pi^0 \rightarrow \pi^+\pi^-\pi^0) = 0.30 \pm 0.055(\text{stat}) \pm 0.068(\text{syst}) \pm 0.029(BR)\%,$$

and, assuming $a_0(980) \rightarrow f_0(980)$ as an underlying mechanism, $BR(a_0^0(980) \rightarrow \pi^+\pi^-) = (2.0 \pm 0.6 \pm 0.4(BR))\%$.

Along with (7), we present the branching ratio which accounts for the component left to the " $f_0(980)$ " signal, $0.94 \lesssim m_{\pi\pi} \lesssim 0.97 \text{ GeV}/c^2$, as asymmetric uncertainty:

$$\frac{BR(f_1 \rightarrow \pi^+\pi^-\pi^0)}{BR(f_1 \rightarrow \eta\pi^+\pi^-)} = 0.86 \pm 0.16_{-0.20}^{+0.70} \%.$$

To summarize, the experimental pattern of the decay, caused presumably by the $a_0(980) \leftrightarrow f_0(980)$ mixing, is badly compatible with the model [18] alone, both on its widths and strength. It suggests another decay mechanism in addition to the $a_0(980) \leftrightarrow f_0(980)$ one.

An upper limit for $f_1(1285) \rightarrow \rho^{+-}\pi^{-+}$ decay is obtained,

$$BR(f_1(1285) \rightarrow \rho^{+-}\pi^{-+}) < 0.31\%,$$

at 95% CL. This limit is compatible with the ISB universal scale [4].

This work supersedes the preliminary results presented at the HADRON-2007 conference [20].

Appendix A.

In non-relativistic Zemach formalism [21] the decay amplitude for the $f_1(1285)\pi$ system in the $J^{PC}M\eta = 1^{++}0+$ state is expressed through the z -component of the cross product constructed from the momenta of f_1 in the Gottfried-Jackson frame and its decay product in the canonical rest frame of f_1 .

For the reference decay chain $f_1 \rightarrow a_0^\pm \pi^\mp, a_0^\pm \rightarrow \eta\pi^\pm$ it reads²:

$$A_{1^{++}0^+} = [\mathbf{p}_{f_1} BW_{f_1}(m_{\pi^+\pi^-\eta}) \times ((\mathbf{p}_\eta + \mathbf{p}_{\pi^+}) BW_{a_0}(m_{\eta\pi^+}) + (\mathbf{p}_\eta + \mathbf{p}_{\pi^-}) BW_{a_0}(m_{\eta\pi^-}))]_z.$$

Under the assumption of $m(\eta\pi^+) \sim m(\eta\pi^-)$ this is proportional to $[\mathbf{p}_{f_1} \times \mathbf{p}_\eta]_z$.

For the decay chain under study, $f_1 \rightarrow f_0\pi^0, f_0 \rightarrow \pi^+\pi^-$,

$$A_{1^{++}0^+} = BW_{f_1}(m_{\pi^+\pi^-\pi^0}) BW_{f_0}(m_{\pi^+\pi^-}) [\mathbf{p}_{f_1} \times \mathbf{p}_{\pi^0}]_z.$$

The aforementioned projection to the canonical z -axis, which is the direction of the beam particle momentum, is convenient to calculate using a rotated coordinate system. It is obtained from the canonical one rotating it by the Treiman-Young angle around the z -axis with successive rotation by the Jackson angle around the new y -axis. Formula (3) results from explicit substitution of the components of three vectors (defined by the momenta of the f_1, η (π^0) and beam) and defining appropriate angles.

This work is supported in part by the Russian Foundation of Basic Research grants 07-02-00631, 10-02-00730.

Open Access This article is distributed under the terms of the Creative Commons Attribution Noncommercial License which permits any noncommercial use, distribution, and reproduction in any medium, provided the original author(s) and source are credited.

References

1. S. Coleman, S.L. Glashow, Phys. Rev. Lett. **6**, 423 (1961).
2. S. Coleman, S.L. Glashow, Phys. Rev. B **134**, 671 (1964).
3. S. Weinberg, Phys. Rev. D **11**, 3583 (1975).
4. S.A. Coon, M.D. Scadron, Phys. Rev. C **51**, 2923 (1995).
5. N.N. Achasov, S.A. Devyanin, G.N. Shestakov, Yad. Fiz. **33**, 1337 (1981).
6. N.N. Achasov, S.A. Devyanin, G.N. Shestakov, Sov. J. Nucl. Phys. **33**, 715 (1981).
7. N.N. Achasov, S.A. Devyanin, G.N. Shestakov, Phys. Lett. B **88**, 367 (1979).
8. C. Hanhart, B. Kubis, J.R. Pelaez, hep-ph/0707.0262.
9. F. Close, A. Kirk, Phys. Lett. B **489**, 24 (2000).
10. V. Dorofeev *et al.*, Phys. Lett. B **651**, 22 (2007).
11. D. Amelin *et al.*, Phys. At. Nucl. **68**, 372 (2005).
12. Yu. Gouz *et al.*, VES Collaboration, AIP Conf. Proc. **272**, 572 (1993).
13. S.I. Bitukov *et al.*, Phys. Lett. B **268**, 137 (1991).
14. S.A. Morrow *et al.*, Eur. Phys. J. A **39**, 5 (2009).
15. M. Ross, L. Stodolsky, Phys. Rev. **149**, 1172 (1966).
16. K. Nakamura *et al.* (Particle Data Group), J. Phys. G: Nucl. Part. Phys. **37**, 075021 (2010).
17. S.L. Glashow, Phys. Rev. Lett. **7**, 469 (1961).
18. N.N. Achasov, G.N. Shestakov, Phys. Rev. D **70**, 074015 (2004).
19. J. Wu, B.S. Zou, Phys. Rev. D **78**, 074017 (2008).
20. V. Dorofeev *et al.*, Eur. Phys. J. A **38**, 149 (2008).
21. C. Zemach, Phys. Rev. B **140**, 97 (1965).

² BW_X stands for a mass-dependent line shape of a resonance X , usually taken as Breit-Wigner function.